Master Equation Analysis of Thermal Activation Reactions: Energy-Transfer Constraints on Falloff Behavior in the Decomposition of Reactive Intermediates with Low Thresholds

W. Tsang,* V. Bedanov,† and M. R. Zachariah

Chemical Science and Technology Laboratory, National Institute of Standards and Technology, Gaithersburg, Maryland 20899

Received: August 25, 1995; In Final Form: December 8, 1995[⊗]

This paper deals with the high-temperature decomposition of reactive intermediates with low reaction thresholds. If these intermediates are created in situ, for example, through radical chain processes, their initial molecular distribution functions may be characteristic of the bath temperature and, under certain circumstances, peak at energies above the reaction threshold. Such an ordering of reaction thresholds and distribution functions has some similarities to that found during chemical activation. This leads to consequences that are essenially the inverse (larger rate constants than those deduced from steady-state distributions) of the situation for stable compounds under shock-heated conditions and hence reduces falloff effects. To study this behavior, rate constants for the unimolecular decomposition of allyl, ethyl, *n*-propyl, and *n*-hexyl radicals have been determined on the basis of the solution of the time-dependent master equation with specific rate constants from RRKM calculations. The time required for the molecules to attain steady-state distribution functions has been determined as a function of the energy-transfer parameter (the step size down) molecular size (heat capacity), high-pressure rate parameters, temperature, and pressure. At 101 kPa (1 atm) pressure, unimolecular rate constants near 10^7 s^{-1} represent a lower boundary, above which steady-state assumptions become increasingly questionable. The effects on rate expressions and branching ratios for decomposition reactions during the pre-steady-state period are described.

Introduction

At sufficiently high temperatures or low pressures, unimolecular decompositions begin to be affected by energy-transfer effects. The physical manifestation of these effects is the decline in rate constants as the pressure is decreased. RRKM calculations,[1] when coupled with a solution of the energy-transfer problem and correct input data, can give a complete picture of the phenomena. Many recent treatments have been concerned with the solution of the steady-state master equation,[2] either directly or through the modified strong collision procedure using an approximation developed by Troe.[3] Obviously, before this steady-state distribution is achieved, there is a period of time where the distribution of the internal energy in the molecules is changing to take into account the decomposition process.[4]

The main concerns of this paper are (1) the determination of the time after which the standard steady-state treatment of unimolecular falloff behavior (leading to a unique time-independent rate constant) becomes valid and (2) the consequences on the rate constants during departures from steady-state behavior. These concerns constitute an especially important problem if one wishes to simulate global chemical processes with programs[21] such as CHEMKIN,[5] since in these codes such phenomena are not considered. It is generally assumed that the time scales for the establishment of the steady state are too short to be of importance. For many systems this is undoubtedly correct. Any effect on branching ratios will, of course, be important regardless of the absolute values of the rate constants. The rate constants, at any time during the redistribution of the population in the internal states of the molecule, are dependent on the nature of the initial distribution and the model for energy transfer. Thus, in extending weak collision effects to the true beginning in time, new elements may be introduced, and it is important to define the problem so as to be able to assess the consequences for chemical kinetic simulations.

A specific example to illustrate this behavior involves the decomposition of aliphatic radicals.[6−8] These reactions are important processes under combustion and pyrolytic conditions[9] and are particularly susceptible to the failure to achieve a steady-state distribution due to their low unimolecular decomposition thresholds. It is well-known[2] that with all other factors being equal lowering the activation energy pushes an unimolecular reaction deeper into the falloff region when the steady-state assumption is applicable. The general situation is illustrated in Figure 1. Clearly, in a number of cases, the positions of the reaction threshold and the equilibrium molecular distribution function make the application of standard steady-state based calculations questionable. Also included in Figure 1 are the steady-state distributions at 1500 K as calculated from the solution of the master equation.[1] The physical phenomena with respect to the molecule is the shifting of the distribution function from the thermal to the steady-state situations. When this is occurring, it is not possible to describe the system in terms of a single rate constant. In this paper we will be concerned with the situation where substantial decomposition occurs during this transient period.

The traditional picture of unimolecular falloff involves a reaction threshold (energy above which reactions can occur) at the high-energy end of the molecular distribution function. The falloff or drop in rate constant is brought about by the more rapid rate of depletion of the higher energy molecules through the reaction in comparison to the rate of activation by collisions. The perturbation on the distribution function is thus small. This situation is the case for allyl at all temperatures and the other radicals at low temperatures. However, for the alkyl radicals, one notes the much broadened distribution functions and the shift of the peaks toward higher energies at high temperatures.

† Permanent address: Institute of Theoretical and Applied Mechanics, Novosibirsk, 630090, Russia.

[⊗] Abstract published in *Advance ACS Abstracts,* February 1, 1996.

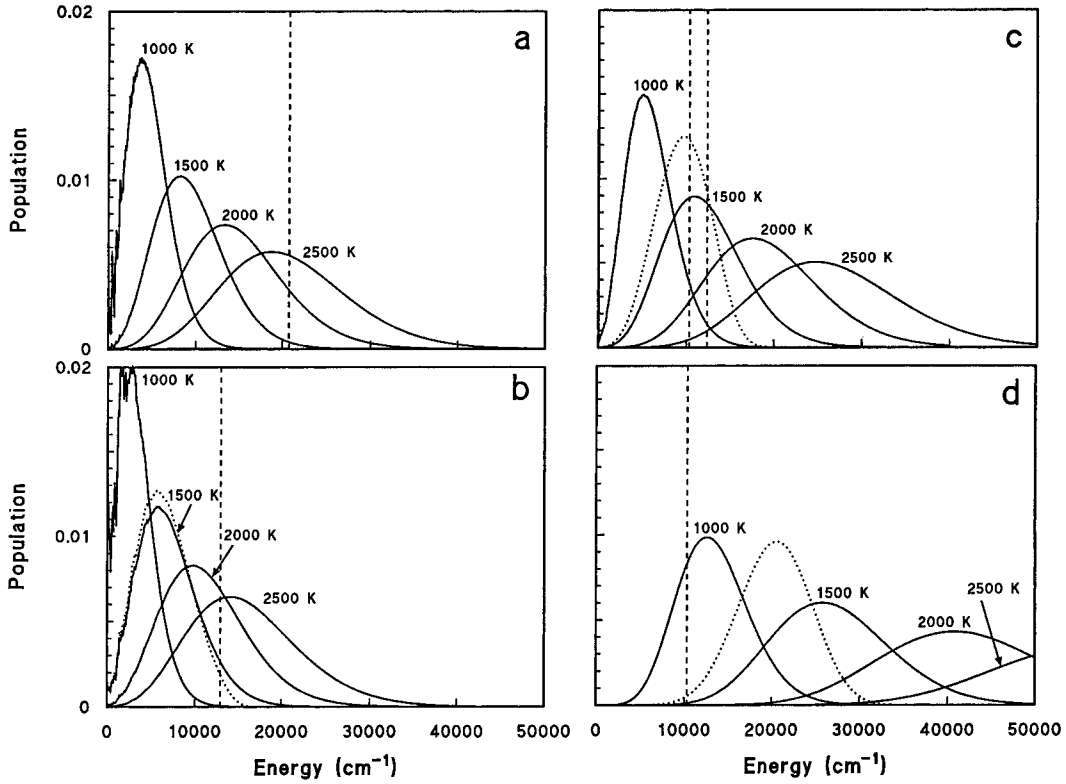

Figure 1. Equilibrium distribution functions at various temperature and steadyhstate distributions at 101 kPa (1 atm) and 1500 K (dotted line) for (a) allyl, (b) ethyl, (c) *n*-propyl, and (d) *n*-hexyl radicals. Vertical lines represent reaction thresholds. The two vertical lines in Figure 3c represent methyl ejection (lower energy) and H-atom ejection (higher energy). Note in (a) the steady-state distribution at 1500 K is virtually the same as the equilibrium distribution at that temperature and is thus hidden.

As a consequence, in a number of cases, the reaction threshold is on the low-energy (wrong) end of the distribution. For these cases, the positions of the high temperature equilibrium distributions and the reaction threshold are more akin to those of a high temperature chemical activation process. In the case of *n*-hexyl at 1500 K, to attain the steady-state distribution from the equilibrium distribution there would have to be large shifts in the distribution function. Note that there is a logical inconsistency in applying the steady-state treatment to these situations. The steady-state treatment will predict infinite stability at the lowest pressures. Obviously, this cannot occur when the energy content of the molecules are above the reaction threshold.

Past Work

Kiefer and co-workers[10] have been able to obtain quantitative measures of the time preceding unimolecular decomposition for a number of intermediate sized polyatomic organic molecules from shock-tube studies with their laser schlieren detection technique. In these cases, the initial internal state of the molecule upon the passage of the shock wave is that characterized by the preshock temperature. The observed induction time relates to the approach from a room-temperature distribution to the steady-state distribution appropriate to a molecule in the falloff regime. These are very important and difficult experiments, because for most molecules the induction time is very short and not easily detectable. However, there are a few systems where induction times can be clearly determined. Barker and King[11] have analyzed the general situation recently. An earlier analysis was carried out by Dove and Troe.[12] It is known that rate of excitation of molecules from their ground vibrational states to upper levels (so as to attain the high temperature distributions) are much slower than those involving the highly excited states of the radicals of interest here. This is due to the smaller density of states at lower energies. Since the nature of the molecule must have a strong influence on the density of states at the lower energy levels, then one would expect to see more variations among molecules when induction time effects are important.

The above is a considerably different problem than that being considered here. Unlike the shock-tube situation, molecules are not largely in their ground vibrational states. Instead as can be seen from Figure 1, highly excited molecules are present. The radicals must all be created through reaction from another molecule that, in all probability, have an internal temperature appropriate to the bath. The formation of a large polyatomic radical, by abstraction, for example, should not lead to an internal temperature for the newly formed radical that is much different than that of the molecule. For example, a *n*-propyl radical would most likely be formed from the decomposition of propane through an abstraction process. Since there is no question that propane, which is much more thermally stable (in the unimolecular sense) than *n*-propyl, will be at the bath temperature, then it follows that the large radical product, *n*-propyl, will probably also be at that temperature (internal as well as translational). Thus unlike the situation with the shock heated gas, the true initial rate constant must be larger than that from the steady-state distribution.

Although for the radicals in question, the selection of an initial reaction distribution that is characteristic of the reaction temperature should be a good approximation, nevertheless, deviations are possible. The newly formed radical does not have to be at the bath temperature. The situation is different for stable molecules under shock heating where the initial states are well specified. The uncertainty in molecular energy is a reflection of the fact that for the period before steady-state distributions are attained rate constants must be dependent on the initial energy distributions of the species in question.

TABLE 1: Properties Relevant to the Calculation of the Unimolecular Decomposition of Some Alkyl Radicals[a]

reaction	A (s^{-1})	E/R (K^{-1})	I (g cm^2)	vibrational frequencies: molecule and transition state (cm^{-1})
$C_3H_5 \rightarrow C_3H_4 + H$ $\sigma = 4.68 \times 10^{-8}$ $\epsilon/R = 299$	$1.5 \times 10^{11} \times T^{0.84}$	30 053	1.6×10^{-39} (1-d) 9.1×10^{-39} (2-d)	mol: 400, 400, 500, 950, 950, 1100, 1100, 1100, 1300, 1300, 1300, 1450, 1450, 3050, 3050, 3100, 3100, 3100 trans state: 200, 300, 500, 1100, 1100, 1100, 1100, 1100, 1300, 1300, 1300, 1450, 1450, 3050, 3050, 3100, 3100
$C_2H_5 \rightarrow C_2H_4 + H$ $\sigma = 4.4 \times 10^{-8}$ $\epsilon/R = 216$	$1.1 \times 10^{10} \times T^{1.04}$	18 504	8.1×10^{-40} (1-d) 3.9×10^{-39} (2-d)	mol: 540, 800, 1140, 1180(2), 1360, 1440, 1400(2), 2840, 2920, 2980, 3040, 3100, 1 f.r. ($I = 1.86 \times 10^{-40}$, symmetry no. = 6) trans state: 500, 700, 800, 1000, 1200, 1400, 1440, 1460(3), 3040(4)
$n\text{-}C_3H_7 \rightarrow C_2H_4 + CH_3$ $\rightarrow C_3H_6 + H$ $\sigma = 5.1 \times 10^{-8}$ $\epsilon/R = 237$	$1.8 \times 10^{12} \times T^{0.3}$ $5.4 \times 10^{11} \times T^{0.46}$	15 252 17 836	2.6×10^{-39} (1-d) 9.2×10^{-39} (2-d)	mol: 180, 330, 530, 960, 980, 990(4), 1100, 1390, 1440(5), 2960(5), 3100(2), 1-f.r. ($I = 2.7 \times 10^{-40}$, symmetry no. = 2) trans state (C−C): 400, 500, 500, 500, 600, 800, 1000(2), 1100, 1400, 1440(5), 2960(5), 3100(2), 1-f.r. rotor ($I = 2.7 \times 10^{-40}$, symmetry no. = 3) trans state (C−H): 300, 500, 580, 900, 1000, 1040, 1100, 1140, 1160, 1180, 1300, 1380, 1400, 1440(2), 1640, 2960(3), 3040(3), 1-f.r. ($I = 4.2 \times 10^{-40}$, symmetry no. = 3, pathway degeneracy = 2)
$n\text{-}C_6H_{13} \rightarrow C_2H_4 + C_4H_9$ $\sigma = 5.95 \times 10^{-8}$ $\epsilon/R = 400$	$1.8 \times 10^{12} \times T^{0.3}$	15 252	5.6×10^{-39} (1-d) 7.0×10^{-38} (2-d)	mol: 180, 330, 530, 960, 980, 990(4), 1100, 1390, 1440(5), 2960(5), 3100(2), [940(3), 1280(3), 1340(3), 1460(3), 2950(6), 320(3), 1000(3), 300(3)], 1-f.r. ($I = 2.7 \times 10^{-40}$, symmetry no. = 2) trans state: 400, 500, 500, 500, 600, 800, 1000(2), 1100, 1400, 1440(5), 2960(5), 3100(2), [940(3), 1280(3), 1340(3), 1460(3), 2950(6), 320(3), 1000(3), 300(3)], 1-f.r. ($I = 2.7 \times 10^{-40}$, symmetry no. = 2)

[a] σ = collision diameter in cm, ϵ/R = Lennard-Jones well depth in K^{-1}. ( ) degeneracy. I-f.r. in g cm^2, [ ] additional frequencies to convert propyl to hexyl.

Bernshtein and Oref[13] have recently published calculations similar to those to be described below for cyclobutane and cyclobutene decomposition at 2000 and 1500 K. The situation they claim to model, stepwise heating (such as obtained from shock-tube experiments) to the reaction temperature, followed by decomposition, is probably not physically meaningful for these stable molecules. In their case[13] the molecules are initially assumed to be at the reaction temperature. However, if the reaction temperature is such that the unimolecular reaction is in the falloff region, then they can never achieve the reaction temperature distribution. Their results are probably most appropriate to fictitious molecules, created in situ, with decomposition properties similar to those used in their calculations. In this framework, there are marked similarities to the present situation and is thus useful as a basis for comparison. Indeed, many of the conclusions drawn here could have been made by Bernshtein and Oref had they applied their analysis to the systems considered here.

Calculational Details

Our procedure is to calculate the time dependent rate coefficients through the solution of the non-steady-state master equation

$$\frac{d\rho_i}{dt} = \omega \sum_j P_{ij}\rho_j - \omega\rho_i - k_i\rho_i \tag{1}$$

or in the matrix form

$$d\rho/dt = J\rho \tag{2}$$

where ρ_i is the (time-dependent) population in the ith level, ω is the collision frequency, k_i is the specific rate constant at a given energy, E, and J is called the relaxation matrix. This is derived from the standard RRKM formula:

$$k(E) = l^+ \frac{G+(E)}{hN(E + E_0)} \tag{3}$$

for a vibrator transition state[2] (equal moment of inertia for molecule and transition state) with the data given in Table 1 where l^+ is the reaction pathway degeneracy, $G^+(E)$ is the sum of states of the transition state at energy E above the reaction threshold, E_0, and $N(E + E_0)$ is the density of states of the decomposing molecule. P_{ij} is the suitably normalized collisional energy-transfer probability where

$$\sum_i P_{ij} = 1 \tag{4}$$

The model of the energy-transfer probability was the standard "exponential down" relation

$$P_{ij} = A_j \exp\left(-\frac{E_j - E_i}{\alpha}\right), \qquad J \geq i \tag{5}$$

where α is a positive parameter governing the amount of energy transferred per collision or the "step size down" and a constant value of 500 cm^{-1} is used. Justification for this approach is given in a subsequent section. The downward and upward transition probabilities are related by the detailed balance

$$P_{ji}f_i = P_{ij}f_j \tag{6}$$

where f_i is the equilibrium distribution function or

$$f_i = \frac{1}{Q} N_i \exp\left(-\frac{E_i}{k_B T}\right) \tag{7}$$

with k_B is the Boltzmann constant, N_i the density of states, and Q the partition function. Note that for the treatment of an extra decomposition channel one needs only add an additional term for decomposition into the master equation. In an earlier paper[14] we described our procedure for solving the master equation. The solution in terms of $\rho_i(t)$ is expressed in terms of the eigenvalues λ_i and eigenvectors S_i of the relaxation matrix J:

$$\rho_i(t) = \sum_j \sqrt{f_i}(S_j)_i e^{\lambda_j t} \sum_k [(S_j)_k/\sqrt{f_k}]\rho_k(0) \tag{8}$$

The time dependent rate constant is given by

$$k(t) = \sum_i k_i\rho_i / \sum_i \rho_i \tag{9}$$

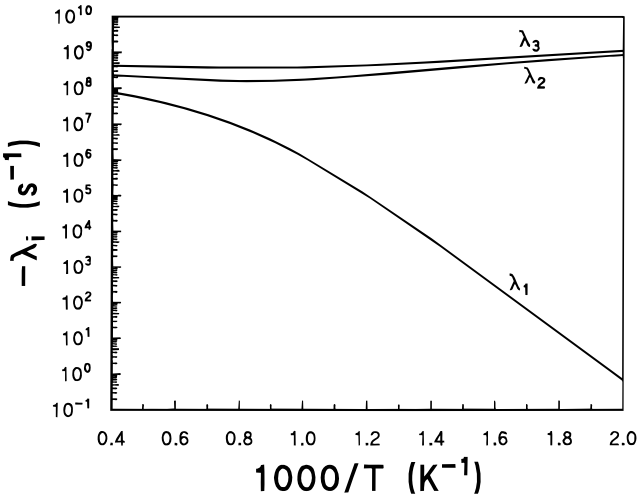

Figure 2. First three eigenvalues as a function of temperature at 101 kPa (1 atm) from the solution of the master equation for *n*-propyl radical decomposition.

Since we are primarily interested in high-temperature combustion processes, most of our calculations are carried out at 101 kPa (1 atm) pressure. For a few cases, we have also investigated the situation below and above this value.

A plot of the eigenvalues obtained as a function of temperature for *n*-propyl decomposition is given in Figure 2. As expected, at lower temperatures where the reaction is in the steady-state regime the largest eigenvalue is the rate constant and is clearly dominating. At other temperatures, other eigenvalues begin to be significant. The deviations from the steady-state behavior (constant rate constant) are a reflection of the increasing contributions from the higher eigenvalues. It was found that the spacing of the higher eigenvalues are similar to that shown for the second and third eigenvalues. However, the dependence of the concentration on the sum of the exponential of the eigenvalues leads to the necessity of only using the first three under all the conditions covered since exclusion of the higher values under our conditions leads to errors of only a few percent in the rate constant.

Molecular Properties

There are no direct experimental data for the kinetics of the decompositions under the conditions covered in this work. Thus it is particularly important to establish the limitations of recommendations and the expected directions and magnitude of deviations from results based on steady-state distributions. Fortunately, there is considerable information on high-pressure rate expressions for these reactions. Important parameters for our calculations are thus available. The specific reactions to be studied, the best estimates for the high-pressure rate expressions, and molecular and transition-state properties are given in Table 1. Also included are the Lennard-Jones parameters[15] that are necessary to place energy transfer on a per collision basis. Although exact values for the properties of the transition state are uncertain, we have chosen values that are similar to the parent molecules with the aim of reproducing the high-pressure rate expressions. For the steady-state situation, it is known that this is all that is required to reproduce falloff behavior. It is important to realize that the results from the steady-state and pre-steady-state distributions are derived on the basis of the same input data. Thus the results for the latter are the logical consequence of those for the former.

A particularly interesting situation is the two-channel decomposition process for *n*-propyl radicals. We are interested in determining how the branching ratios will be affected by the non-steady-state distributions being studied. The allyl radical decomposition has a relatively high activation energy and thus represents the upper reaction threshold limit for these calculations. The description of the decomposition of the *n*-hexyl radical treated here is for the hypothetical situation where only β C−C cleavage is of importance. It is being studied to obtain guidance regarding the behavior of a large molecule (or more generally, the effect of increasing heat capacity or entropy). Thus we have selected its vibrational frequencies and those of its transition states for decomposition in such a fashion so that they will produce the exact rate expression as that for β C−C bond fission in the *n*-propyl decomposition system. It can be seen from Figure 1 that the immediate consequence of increasing the heat capacity or entropy per molecule is to broaden the distribution and move the peak of the distribution toward higher energies. The actual mechanisms for 1-hexyl radical decomposition involves isomerization coupled with β C−C bond cleavage leading to a variety of smaller alkyl radicals and olefins. A more complete discussion of the general problem will be presented in the near future.

For the specification of energy-transfer processes, we have selected a constant value of 500 cm^{-1} for the step size down, α. This choice was based on the analysis of a great deal of existing data that cover wide temperature ranges.[16] For example, for helium as the collider, the experimental evidence for a radical such as ethyl is a linear dependence of the form of $0.25T$ cm^{-1} over the temperature range 300−1100 K. The data from high-temperature thermal decomposition studies in the 1500−3000 K range, in argon or krypton,[4] usually leads to a 500 cm^{-1} value. For larger polyatomics as colliders, the existing data suggest very little temperature dependence and values in the 500−1000 cm^{-1} range. In this application, the concern is with environments such as those found in materials processing or combustion in the 1000−2000 K range. For combustion, important contributors for energy transfer, along with N_2, are polyatomic species such as carbon dioxide and water. For material processing, an inert atomic gas such as argon is frequently used as a buffer. The errors introduced by the use of a constant step size down should not be large, and we have indicated the range of possibilities in two of the subsequent figures. Except for allyl, the structure of all the radicals are extremely "loose" in the sense that they contain at least one free rotor and other low-frequency vibrations. This should facilitate energy transfer. The step size down used here, 500 cm^{-1}, is not inconsistent with the direct measurements of Hippler and Troe[17] and Barker[18] and their co-workers on the deexcitation of vibrationally hot large polyatomic molecules. Some error is introduced by neglect of the temperature dependence. The direct studies have shown a linear dependence on the internal energy of the molecule and a more formally correct approach would be to introduce this into the calculations. As can be seen in Figures 4c and 5b the results are not particularly sensitive to small changes in the step size parameter.

Results

Figure 3 gives a typical result from the calculations. The example used here is for *n*-propyl radical decomposition at 2000 K and at 101 kPa (1 atm) pressure. As a result of the initial thermal distribution at this temperature, rate constants for thermal decomposition are very high. Decomposition and collisions with the bath molecules will in time bring the rate constants to the steady-state value. Figure 3b shows the extents of decomposition at various times. It can be seen that in this case a substantial quantity of the radical has decomposed during

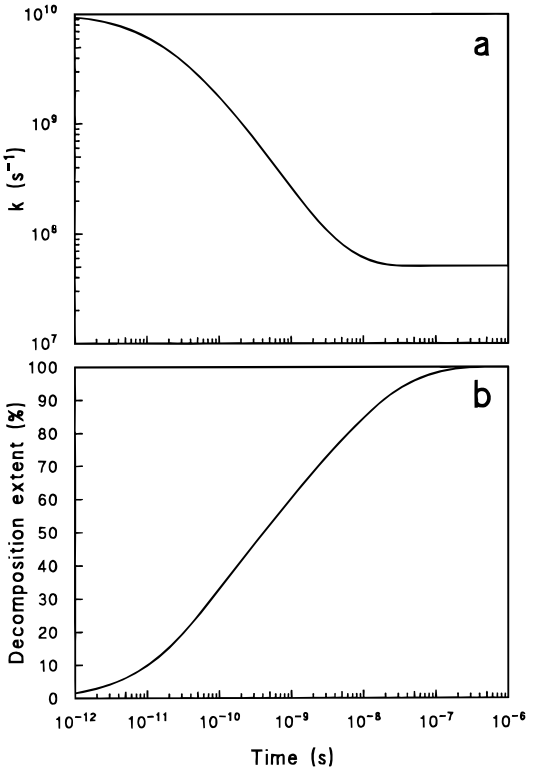

Figure 3. (a) Rate constants versus time and (b) extent of decomposition versus time for C−C bond cleavage during *n*-propyl radical decomposition at 2000 K and 101 kPa (1 atm).

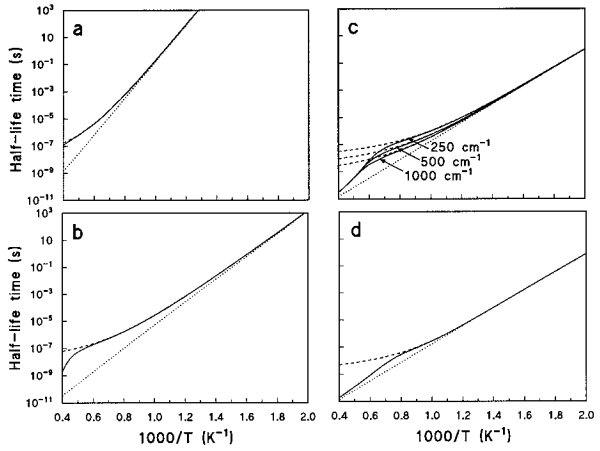

Figure 4. Half-lives versus temperature for the decomposition of allyl (a), ethyl (b), propyl (c), and *n*-hexyl (d) radicals at 101 kPa (1 atm) pressure. Dotted lines are high-pressure values. Dashed lines are for steady-state distribution. Solid lines are results from solution full master equation. Also included in Figure 4c are data for *n*-propyl decomposition at various labeled step sizes down.

the time period when it is not possible to talk about an invariant decomposition rate "constant".

On the other hand, it is still possible to identify the half-life of the molecule at various pressures as a function of temperature. The data can then be presented in a visual format that is useful for obtaining physical insights. Appropriate curves, on the basis of the exact solution of the master equation, for the four molecules under consideration can be seen in Figure 4. The general picture for a pressure of 101 kPa (1 atm) is as follows. At the lowest temperatures one is at or very close to the high-pressure limit. The reaction is in fact occurring out of an equilibrium distribution. As the temperature is increased, one enters into the falloff region, and the half-life becomes larger than those at the high-pressure limit. Here the process is still characterized by a constant distribution function, but it is no longer that for the equilibrium situation (that leads to high-pressure rate constants). However, as the temperature is further increased, one enters into the non-steady-state distribution region and the half-life now begins to go back to the high-pressure value. One thus obtains for every pressure a rather odd half-life versus temperature plot with the additional caveat that when there are deviations from the steady-state distributions a time-independent rate constant can no longer be defined.

In the context of the molecules being considered, Figure 4a shows that for the most stable radical, allyl, the results are in the steady-state region for temperatures up to 2500 K. The time to achieve the steady-state distribution is too small to make any difference, and the usual falloff calculations give adequate results. Figure 4b contains data for the ethyl radical, where deviations from the steady-state behavior commence at about 2000 K. In this case the barrier is about 160 kJ/mol. Figure 4c contains data for *n*-propyl radical decomposition and is based on the total rate constant for decomposition. The major contribution is from the low-energy C−C bond-breaking process. The smaller contributions from the upper channel will be discussed below. The onset of deviations from steady-state behavior is now lowered to near 1500 K at 101 kPa (1 atm) pressure or a temperature range which are of concern for combustion and materials-processing contexts. Although the molecular sizes (as reflected in the heat capacities or entropies) are somewhat different, what is being observed is the influence of decreasing activation energies. In the present study the activation energies range from approximately 250 kJ/mol for allyl to near 125 kJ/mol for *n*-propyl and *n*-hexyl. Figure 4c also contains data for a number of step sizes down (or α from eq 5). This is for the purpose of assessing effects arising from possible uncertainties in this parameter. It can be seen that, as expected, the different step sizes affect the steady-state rate constant. However, from the magnitudes of the deviations and the temperatures where they occur, the consequences arising from varying step sizes does not appear to be very large at 101 kPa (1 atm) pressure. Note that at the highest temperatures the effects disappear. We believe that the step sizes considered here cover all the possibilities with respect to collisional energy transfer and that the spread of results is a good estimate of the sensitivity of the calculations to this parameter. Finally, Figure 4d gives the results for the decomposition of *n*-hexyl through β C−C bond cleavage. As expected, the falloff behavior at the same pressure (101 kPa or 1 atm) and step size (500 cm^{-1}) is somewhat less pronounced than the situation with *n*-propyl radical. The temperature where deviation from steady state occurs is lower than that for *n*-propyl and the half-lives rapidly approach the limiting high-pressure rate constants again as the temperature is increased. Thus, the region where there is a major departure from the high-pressure limit is reduced. Finally, it is important to note the consequences, in terms of half-lives for ethyl, *n*-propyl, and *n*-hexyl radicals, of not taking into account the non-steady-state distribution behavior at the highest temperatures considered.

It should be emphasized again that the results given above are based on the assumption that the radicals are at the bath temperature. In principle, one could have any initial distribution, subject only to the conservation laws. Thus a band of half-lives, bounded by the high-pressure and steady-state rate constants are in fact possible. Note again that we have resorted to considering the half-life because in the non-steady-state condition the rate "constants" are in fact time varying functions.

Figure 5 gives the pressure dependence for the half-life of the decomposing species at 1000 and 1500 K for decomposition

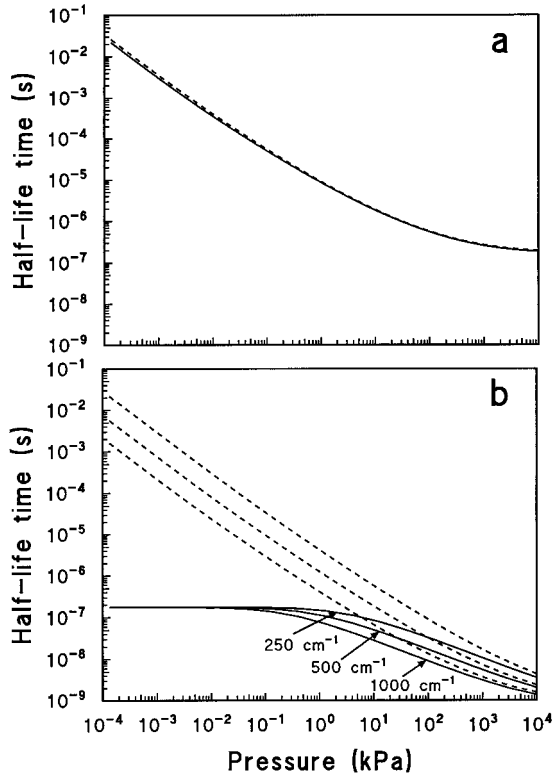

Figure 5. Dependence of half-lives on pressure at 1000 K (a) and 1500 K (b) for C−C bond cleavage during *n*-propyl radical decomposition. Numbers refer to step sizes at 1500 K. Dotted lines are results for steady-state distributions. Solid lines are from complete master equation solution.

through β C−C bond fission for *n*-propyl radical. The results in Figure 5a shows that at 1000 K steady-state behavior occurs even at the lowest pressures. However, the situation changes considerably at 1500 K (Figure 5b). As expected, at the higher pressures, the results are very close to those based on the steady-state assumptions. However as the pressure is decreased, the half-life no longer increases. Instead, it approaches a constant value that is larger than the high-pressure half-life. This result is due to the loss through decomposition of the high-energy tail of the distribution. Since there are insufficient collisions to equilibrate the molecule with the bath, the distribution function is shifted away from the high-pressure values. This situation is very much akin to that found during chemical activation.[19] Of particular importance is the demonstration that, at 1500 K, a low-pressure limit in the conventional unimolecular decomposition sense does not exist. Fortunately, the results in Figures 4c and 5b suggest that the onset of non-steady-state behavior is quite sharp as a function of temperature. Thus, until the onset temperature the use of a low-pressure limit would appear to be quite valid. Also included in Figure 5b are the changes with pressure of the half-life for various step sizes down. The general effect is similar to that for the various step sizes used in Figure 4c. Note that in both cases there is only a narrow region where the selection of step sizes becomes important. This is in contrast to the results from the steady-state treatment (also in Figure 5b) where the unimolecular rate constants continuously decrease with pressure.

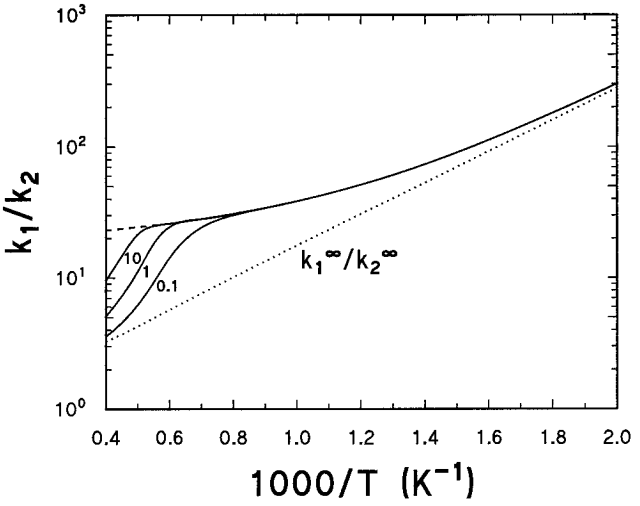

Figure 6. Relative rate constants for C−C bond breaking versus C−H bond breaking in *n*-propyl radical decomposition as a function of temperature at different times (labeled in terms of multiples × half lifes at 101 kPa (1 atm)). Dotted line: high-pressure limits. Dashed lines: based on steady-state assumption. Solid lines: full master equation solution.

Figure 6 demonstrates the consequences on the branching ratios for β C−H and C−C bond cleavage as one approaches and enters into the non-steady-state region at 101 kPa (1 atm). In this case, it is necessary to consider the ratio of rate constants, since the half-life of the molecule is not appropriate for this situation. The calculations show that in the time-dependent region even the ratio of rate constants cannot be treated as constant at a particular temperature. Hence we present results for the ratio of rate constants at multiples of the half-life. At the lowest temperatures, the results are all near the high-pressure limit. At higher temperatures, the ratio begins to deviate from the high-pressure ratio in the direction of decreasing contributions from the upper channel (in comparison to the high-pressure values). In the non-steady-state region (1500−2000 K) the ratio of rate constants once again approaches the high-pressure situation regarding contributions from the upper channel.

Finally, in Figure 7 we give results for cyclobutane and allyl radicals at the very high temperatures (>3000 K) where nonsteady effects are of importance. Aside from the purely molecular properties, the high-pressure rate expressions differ by approximately 2 orders of magnitude in *A* factor (4×10^{15} s^{-1} for cyclobutane and 6×10^{13} s^{-1} for allyl). The activation energies are virtually the same. The input data for cyclobutane decomposition are those of Bernshtein and Oref[13] and summarized in Table 2. However, we have changed the reaction threshold to 247 from 261.5 kJ/mol. This change is needed because Bernshtein and Oref did not take into account the temperature dependence of the *A* factor. With the parameters in Table 2 we can now reproduce the experimental high-pressure rate expression. Allyl is of course a somewhat smaller molecule (smaller heat capacity and entropy). Due to the large activation energies for these decomposition reactions, interesting effects

TABLE 2: Properties Relevant to the Calculation of the Unimolecular Decomposition of Cyclobutane[a]

reaction	*A* (s^{-1})	*E*/*R* (K^{-1})	*I* (g cm^2)	vibrational frequencies: molecule and transition state
$C_4H_8 \rightarrow 2C_2H_4$	$2 \times 10^{13} \times T^{0.65}$	30800	1.4×10^{-38} (1-d)	mol: 197, 627, 741, 750(2), 900(2), 926, 1000(2), 1220(4), 1260(4), 1445(4), 2890(4), 2950(2), 2980(2)
$\sigma = 4.34 \times 10^{-8}$				
$\epsilon/R = 175$			7.9×10^{-39} (2-d)	trans state: 150, 350(2), 380, 600(2), 740(2), 850, 898, 1000, 1100(2), 1250(2), 1260(2), 1445(4), 2980(8)

[a] σ = collision diameter in cm, ϵ/R = Lennard-Jones well depth in K^{-1}.

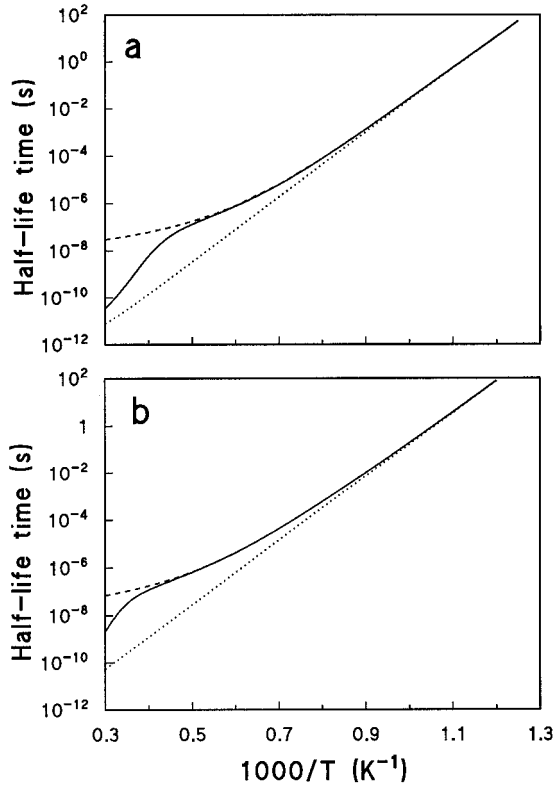

Figure 7. Half-lives versus temperature for the decomposition of cyclobutane (a) and allyl radical (b) at 101 kPa (1 atm). Dotted lines: high-pressure rate constants. Dashed lines: steady-state solution of master equation. Solid lines: full solution of master equation.

are manifested only above 2500 K. The data in Figure 7 show that falloff behavior is larger for cyclobutane. This is a consequence of the larger *A* factor overcoming the effect of the smaller molecular size or heat capacity. In addition, the approach to non-steady-state behavior begins somewhat earlier and the return to the high-pressure rate constants is more rapid for cyclobutane.

Discussion

The initial impetus for this work was the need to determine the limits of applicability of the steady-state approximation for unimolecular decomposition at high temperatures appropriate to materials processing and combustion applications and to estimate the nature of the deviations from the steady-state approximation. In the course of this work, it became clear that the dependence on the initial distribution requires drawing a distinction between (1) molecules that are formed in the course of reactions and (2) those that are present before the initial temperature perturbation, as in shock-wave studies. For the first case, these calculated deviations from the steady-state distributions bring rate constants for decomposition closer to those at the high-pressure limit. Thus energy transfer effects reduce falloff. This effect becomes manifest at the highest temperatures and lowest pressures, where falloff effects are usually expected to be most important. Thus at any temperature and pressure the high-pressure rate constants and those derived on the basis of a steady-state distribution form the boundaries for possible rate constants. This is contrast to the shock tube situation where in the non-steady-state region unimolecular decomposition rate constants are smaller than the steady-state values.

From the curves in Figure 4 it appears that at 101 kPa (1 atm) pressure it is necessary to begin considering non-steady-state distribution effects when unimolecular rate constants are in the 10^7-10^8 s^{-1} range or at this pressure, 1000−10000 collisions. This result is consistent with those in Figure 2, where at these values of the rate constants the first eigenvalue (which is the steady-state rate constant) is no longer as dominating in comparison to the other eigenvalues. It is interesting that this boundary appears to be only weakly dependent on all the parameters that have been varied. We are uncertain of the causes for this constancy. It does offer a very simple criteria for making decisions on when non-steady-state effects become important. An alternative although weaker criterion for considering the onset of non-steady-state behavior are when *E*/*RT* values less than 10. However, the results in Figure 4 suggest that for molecules with larger entropies or heat capacities, a higher onset value of *E*/*RT* may be more applicable. For most high-temperature combustion or materials processing applications, it would appear that with normal *A* factors and activation energies above the 160 kJ/mol range, the steady-state solutions of the master equation will give acceptable results. On the other hand for activation energies in the 120 kJ/mol range, as in case of *n*-propyl radicals, the onset of the induction time begins near 1500 K.

The results for the branching ratios (Figure 5) from radical decomposition can be considered in the same manner as that for the half-lives discussed earlier. As expected, the lower temperature results are consistent with reactions occurring out of an equilibrium distribution. Hence the upper channel is discriminated against by the activation energy differences. As one goes to higher temperatures, the consequences on the ratio of rate constants arising from the decrease in the importance of the activation energy is offset by the discrimination against reaction from the upper channel, since the nonequilibrium steady-state distribution has its high-energy tail truncated by reaction. At the highest temperatures considered, where the reaction enters the non-steady-state regime, the decomposition is now so fast that it reflects more of its initial equilibrium distribution. In the case of propyl radical the ejection of hydrogen atom regains its importance.

The results for *n*-hexyl radicals are especially interesting because together with the data on *n*-propyl they illustrate the effect of heat capacity or entropy. As such, they may be very suggestive of the situation when one deals with real fuels or feedstocks (larger molecules). It is known that molecules with high entropies or heat capacities show lessened falloff behavior in comparison with those having smaller entropies or heat capacities if the rate expressions for decomposition are similar. This is because the limiting low-pressure rate constant must increase with heat capacity or entropy since it is related to the density of states of the molecule. Thus if the limiting high-pressure rate constant is unchanged, then the result is a falloff curve that is translated toward lower pressures.

For molecules with higher heat capacities or entropies (or larger molecules), the distribution function is shifted to higher energies and broadened. The consequence as seen in Figure 1d, where even at relatively low temperatures the reaction threshold for *n*-hexyl radical is now behind the peak of the initial thermal distribution. Thus in the context of similar energy transfer effects (on a per collision basis) an earlier onset of non-steady-state behavior is not unexpected for larger molecules, since there are more steps to be taken. Indeed one can well envision the situation where for a sufficiently large molecule falloff effects will nearly disappear, and it will be possible to use the high-pressure rate constants for all simulation purposes. In the case for *n*-hexyl radical, the overall effect at atmospheric pressure is no more than a factor of 3. Unfortunately, for

smaller molecules, the effects that we have noted here adds another layer of necessary calculations to the estimation of rate constants.

Since low activation energies are among the most important indicators of the need to consider nonsteady solutions to be master equation, one would expect that the effects described here will be manifested even more strongly in the decomposition of radicals containing hetero groups or the isomerization of various radicals and diradicals.[20] The reaction thresholds for such processes are frequently in the 40−90 kJ/mol range. Of course, reversible isomerizations have certain unique problems,[14] and it would be extremely interesting and important to consider the situation where such processes are coupled with decomposition. This is the actual situation with *n*-hexyl radicals. We are currently carrying out studies on such systems.

The effects that have been described here represent the ultimate consequences of the treatment of unimolecular decompositions (in the context of RRKM theory) under weak collision constraints. It should be mentioned again that the results are applicable only to a particular scenario. Although plausibility arguments have been given, there are certainly other possibilities. For example, if the radicals were formed from thermal decomposition processes, then one may have to consider the non-steady-state behavior of the molecule and that of the "cold" radicals that are formed during this time.

It is possible to convert the half-lives plotted in Figure 4 to rate constants. This approach would be valid, however, only if unimolecular decomposition is the predominating reaction in the pre-steady-state region. In the case of branching ratios we note that the spread of values are much smaller than those of the rate constants. Finally, it should be noted that the temperature dependence of the half-lives given here are such that the modified Arrhenius form is probably inadequate.

It is difficult to envision how one can carry out experiments to verify the results of this work, although as indicated earlier the conditions necessary for their occurrence, higher temperatures, and lower pressures are present in important technological applications. There is the need for microsecond or submicrosecond detection capability and the capability of generating the species by thermal techniques and is thus a severe experimental challenge. Nevertheless, such measurements will represent an ultimate consistency check on the whole structure of present day procedures for determining unimolecular decomposition behavior. In terms of data for simulations it is clear that the phenomena must be treated on an individual basis. At the present time the only generalizations are for the conditions where the effects begin to become important.

Acknowledgment. The contributions of W.T. to this work was carried out with the support of the Department of Energy, Division of Basic Energy Sciences.

References and Notes

(1) Gilbert, R. G.; Smith, S. C. *Theory of Unimolecular and Combination Reactions*; Blackwell: Oxford, 1990.

(2) Robinson, P. J.; Holbrook, K. A. *Unimolecular Reactions*; Wiley-Interscience: New York, 1972.

(3) Gilbert, R. C.; Luther, K.; Troe, J. *Ber. Bunsen-Ges. Phys. Chem.* **1983**, *87*, 190.

(4) Tsang, W.; Kiefer, J. H. *Unimolecular Reactions of Large Polyatomic Molecules over Wide Ranges of Temperatures*; Liu, K., Wagner, A., Eds.; World Scientific: Singapore, in press.

(5) Kee, R. J.; Miller, J. A.; Jefferson, T. H. CHEMKIN: A General-Purpose, Problem Independent, Transportable, Fortran Chemical Kinetics Code Package; SAND80-8003, Sandia National Laboratories, 1989.

(6) Feng, Y.; Niiranen, J. T.; Bencsura, A.; Knyazev, V. D.; Gutman, D.; Tsang, W. *J. Phys. Chem.* **1993**, *97*, 871.

(7) Tsang, W.; Walker, J. A. *J. Phys. Chem.* **1992**, *96*, 8378.

(8) Tsang, W. *J. Phys. Chem. Ref. Data* **1988**, *17*, 887.

(9) Hucknall, D. J. *Chemistry of Hydrocarbon Combustion*; Chapman and Hall: London, 1985.

(10) Kiefer, J. H.; Kumaran, S. S.; Sundaram, S. J. *J. Chem. Phys.* **1993**, *99*, 3531.

(11) Barker, J. R.; King, K. Vibrational Energy Transfer in Shock Heated Norbornene. *J. Chem. Phys.*, submitted.

(12) Dove, J. E.; Troe, J. *Chem. Phys.* **1978**, *35*, 1.

(13) Bernshtein, V.; Oref, I. *J. Phys. Chem.* **1993**, *97*, 6830.

(14) Bedanov, V. M.; Tsang, W.; Zachariah, M. R. *J. Phys. Chem.*, in press.

(15) Reid, R. C.; Prausnitz, J. M.; Poling, B. E. *The Properties of Gases and Liquids*; McGraw-Hill Book Company: New York, 1987.

(16) Tsang, W. *Combust. Flame* **1989**, *78*, 71.

(17) Hippler, H.; Troe, J. Recent Direct Studies of Collisional Energy Transfer om Vibrationally Excited Molecules in the Ground Electronic State. *Adv. Gas Phase Photochem. Kinet.* Ashford, M. N. R., Baggott, I. E., Eds.; Roy. Soc. Chem.: Letchworth, Hets. SG61HN, England, 1990.

(18) Barker, J. R.; Tosselli, B. M. *Int. Rev. Phys. Chem.* **1993**, *12*, 305.

(19) Kohlmaier, G. H.; Rabinovitch, B. S. *J. Chem. Phys.* **1963**, *38*, 1692.

(20) Benson, S. W.; O'Neal, H. E. Kinetic Data on Gas Phase Unimolecular Reactions; NSRDS-NBS 21, US Government Printing Office, Washington DC 20402, 1970.

(21) Certain commercial materials and equipment are identified in this paper in order to specify adequately the experimental procedure. In no case does such identification imply recommendation or endorsement by the National Institute of Standards and Technology, nor does it imply that the material or equipment is the best available for the purpose.

JP9524901